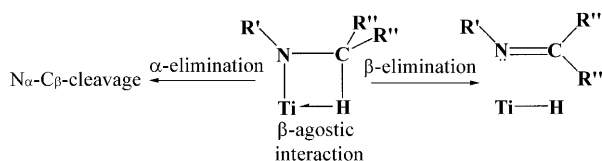


On the Nature of Agostic Interactions in Transition-Metal Amido Complexes**

Wolfgang Scherer,* David J. Wolstenholme, Verena Herz, Georg Eickerling,* Andreas Brück, Paul Benndorf, and Peter W. Roesky*

Dedicated to Professor Herbert W. Roesky on the occasion of his 75th birthday

β -hydrogen (β -H) elimination is a rarely documented phenomenon for transition-metal amido complexes (Scheme 1).^[1] The first directly observable example of a β -H elimination



Scheme 1. Two possible elimination pathways for transition-metal amido complexes containing β -agostic interactions.

involving a monomeric late-transition-metal amido complex, $[\text{Ir}(\text{PPh}_3)_2(\text{CO})\{\text{N}(\text{CH}_2\text{Ph})\text{Ph}\}]$ (**1**), was reported by Hartwig in 1996.^[1a] Surprisingly, the β -H elimination in **1** occurs slowly (depending on the concentration of added phosphine) and requires relatively high temperatures (110 °C in toluene) to obtain stable *N*-phenyltoluenimine and the hydrido species $[\text{Ir}(\text{PPh}_3)_2(\text{CO})\text{H}]$ (**1a**).

Hartwig concluded that “ β -H elimination of late metal amides can be much slower than elimination of the corresponding alkyl complexes”.^[1a] In general, it is assumed that the potential energy surface (PES) of the β -H elimination process in transition-metal alkyl complexes involves intermediates in which β -agostic interactions occur.^[2] Hence, the

reduced β -H elimination activity in amido compared to alkyl complexes may be due to the enhanced ability of alkyl systems to form pronounced β -agostic interactions even in the ground state. This might explain “the different mechanistic features detected for amido, alkoxo and alkyl derivatives which makes it difficult to directly compare their tendencies to undergo β -elimination reaction”^[1k] even in related complexes. Therefore, we have compared the structural and electronic characteristics of various d^0 alkyl and amido benchmark complexes exhibiting deformations resulting from β -agostic interactions in their ground-state structures (Figure 1). This study should provide further insight into the control parameters for elementary β -H elimination processes.

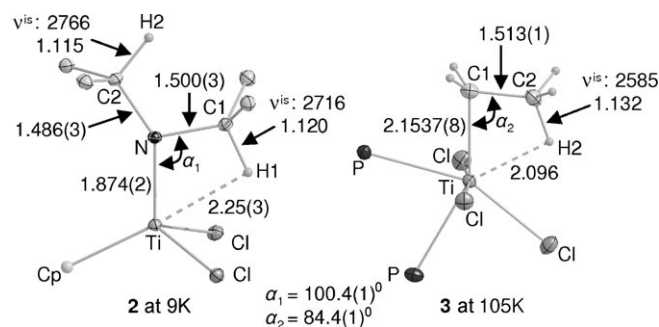


Figure 1. ORTEP representations (thermal ellipsoids set at 50% probability level) for the structural fragments of **2** at 9 K and of **3** at 105 K containing the agostic interaction. Selected bond lengths [Å] and angles [°] are given together with the experimental wavelengths ν^{vis} . C–H distances were not refined as they were calculated from isolated C–H stretching frequencies ν^{is} .

Figure 1 highlights the salient structural features for the reference d^0 titanium amido and titanium alkyl complexes, $[\text{CpTi}(\text{iPr}_2\text{N})\text{Cl}_2]$ (**2**)^[3a] ($\text{Cp} = \text{C}_5\text{H}_5^-$) at 9 K^[3b] and $[\text{EtTiCl}_3(\text{dmpe})]$ (**3**)^[3c] ($\text{dmpe} = (\text{CH}_3)_2\text{PCH}_2\text{CH}_2\text{P}(\text{CH}_3)_2$) at 105 K. Alkyl complexes containing β -agostic interactions are typically characterized by acute $\angle\text{MC}_\alpha\text{C}_\beta$ angles,^[2c] while $\angle\text{MN}_\alpha\text{C}_\beta$ angles smaller than the expected 120° in combination with short $\text{M}\cdots\text{H}_\beta$ distances have been suggested as indicators of amido groups involved in β -agostic interactions.^[3a,4] On the basis of these structural criteria, **2** reported by Pupi et al.,^[3a] has one of the smallest $\angle\text{MN}_\alpha\text{C}_\beta$ angles and shortest $\text{M}\cdots\text{H}$ distances observed to date for an amido species with a β -agostic interaction (see the Supporting Information). The above geometrical definition of an agostic

[*] Prof. Dr. W. Scherer, Dr. D. J. Wolstenholme, Dipl.-Phys. V. Herz, Dr. G. Eickerling, Dr. A. Brück
Institut für Physik, Lehrstuhl für Chemische Physik und Materialwissenschaften, Universität Augsburg
86135 Augsburg (Germany)
Fax: (+49) 821-598-3227
E-mail: wolfgang.scherer@physik.uni-augsburg.de
georg.eickerling@physik.uni-augsburg.de

Dipl.-Chem. P. Benndorf, Prof. Dr. P. W. Roesky
Institut für Anorganische Chemie
Karlsruhe Institute of Technology (KIT)
Engesserstrasse 15, 76131 Karlsruhe (Germany)
Fax: (+49) 721-608-4854
E-mail: roesky@kit.edu

[**] This work was supported by the DFG (SPP1178) and NanoCat (an International Graduate Program within the Elitenetzwerk Bayern). D.J.W. thanks the Alexander von Humboldt foundation for a postdoctoral fellowship. We thank Prof. Jun Okuda for providing us unpublished NMR data of complex **4**.

Supporting information for this article is available on the WWW under <http://dx.doi.org/10.1002/anie.200905463>.

interaction accounts for most of the alkyl and amido complexes containing agostic interactions, but separates the nature of the phenomenon and the driving force behind it from its observable chemical implications.^[2c] Indeed, a closer inspection of **2** reveals that concerted β -H elimination processes involving activated β -C-H bonds and agostic $M\cdots H-C$ interactions appear hindered in d^0 transition-metal amido complexes compared to their alkyl congeners (Figure 1). Clearly, the pronounced π -bonding character of the coordinating N atom hinders any hyperconjugative electron delocalization of the M-N bonding electrons which is essential for establishing strong β -agostic interactions.^[2c,3c] Both our low-temperature X-ray study at 9 K and density functional theory (DFT) calculations show that the agostic iPr_2N moiety of **2** displays no imine character but rather an activated N-C bond of 1.500(3)/[1.497 Å] compared with its non-agostic $iPrN$ fragment (N-C2 = 1.486(3)/[1.478 Å]),^[5] values obtained by DFT calculations employing the ZORA-Hamiltonian at the BP86/TZ2P level of approximation^[6] are given in square brackets. In contrast, the benchmark alkyl complex **3** has a $C_\alpha-C_\beta$ bond length of 1.513(1) Å, which is shorter than standard C-C single bonds in systems without agostic interactions (e.g. 1.526(11) Å in [EtTiCl₃]).^[7] These results are in line with the partial olefinic character of an agostic ethyl group (Figure 1). A literature survey (see the Supporting Information) has revealed that the observed lengthening of the $N_\alpha-C_\beta$ bond is a characteristic feature of agostic amido moieties which thwarts the β -H elimination process by hindering the amido ligand from attaining an imine-type character (Scheme 1).

The small extent of the β -H activation provides another argument for the hindrance of β -H elimination in **2**. Indeed, our DFT calculations predict only a subtle elongation of the C1-H1 bond of the agostic methine group relative to the standard C2-H2 bond in **2** ($\Delta r(C-H) = 0.004$ Å). This theoretical result is supported by the experimental infrared data for **2** which reveal two isolated stretching frequencies, $\tilde{\nu}(v^{is})$,^[8] for the agostic ($\tilde{\nu}(v^{is}) = 2716$ cm⁻¹) and non-agostic ($\tilde{\nu}(v^{is}) = 2766$ cm⁻¹) methine groups. McKean's empirical correlation^[8] linking $r_0(C-H)$ bond lengths to $\tilde{\nu}(v^{is})$ values predicts a marginal bond length difference of 0.005 Å between the $C_\beta-H$ bonds involved in agostic interactions (C1-H1) and non-agostic $C_\beta-H$ bonds (1.120 and 1.115 Å, respectively), in excellent agreement with the corresponding DFT calculations (1.106/1.102 Å). A direct comparison of the $\tilde{\nu}(v^{is})$ values of **2** with the corresponding one derived from the [CHD₂CD₂TiCl₃(dmpe)] isotopologue of **3** ($\tilde{\nu}(v^{is}) = 2585$ cm⁻¹)^[8d] supports our hypothesis that β -H activation is in general significantly weaker in d^0 amido complexes containing agostic interactions than in the corresponding d^0 alkyl complexes (Figure 1).

In general, β -H activation is linked with a significant redistribution of the bonding electron density upon the development of a $M\cdots H_\beta-C$ interaction.^[2c,3c] This electronic redistribution should be reflected by decreased $^1J_{C-H}$ coupling constants and a high-field shift of the agostic proton on the ¹H NMR scale.^[2] The ¹H variable-temperature NMR spectroscopic investigation of **2** in [D₈]toluene exhibits one broad singlet for the methine protons ($\delta = 4.72$ ppm) at room

temperature. Upon cooling to 178 K, the peak arising from the methine protons broadens and splits into two broad singlets at $\delta = 2.33$ (non-agostic) and 6.77 ppm (agostic proton). The splitting of the methine signal indicates the presence of a static β -agostic interaction which arises from the freezing of the rotation of the iPr_2N moieties about the Ti-N and N-C _{β} bonds at lower temperatures. The activation parameters for the overall process were determined from VT NMR experiments ($\Delta H^\ddagger = (37.4 \pm 1.0)$ kJ mol⁻¹, $\Delta S^\ddagger = (-20 \pm 193)$ J mol⁻¹ K, $E_A = (39.3 \pm 1.0)$ kJ mol⁻¹), in qualitative agreement with our DFT calculations (see the Supporting Information). The two methine groups can also be distinguished from their gated ¹³C NMR spectra at 178 K, which show two doublets at $\delta = 50.0$ ($^1J_{C-H} = 120.2$ Hz) and $\delta = 59.1$ ppm ($^1J_{C-H} = 134.7$ Hz). A comparison with other experimental ¹H shifts of agostic methine protons in the related amido complexes **4-6**^[9] reveals a clear correlation between the Ti \cdots H separation and the chemical shifts (Figure 2 and Table 1). Accordingly, a relaxed PES scan (Figure 2 and Table 1) of **2** correlates the shortening of the Ti \cdots H _{β} distance with a positive (downfield) shift of the agostic proton despite its formally increasing hydridic character, consistent with the observed downfield shifts found in **3**.^[12] This situation is in agreement with the observation that also classical d^0 titanium hydrides exhibit pronounced downfield shifts of the terminal hydrogen atom.^[9c,d] Analysis of the individual diamagnetic (σ^d) and paramagnetic (σ^p) contribution to the isotropic shielding $\sigma = \sigma^d + \sigma^p$ shows that the downfield ¹H NMR shifts

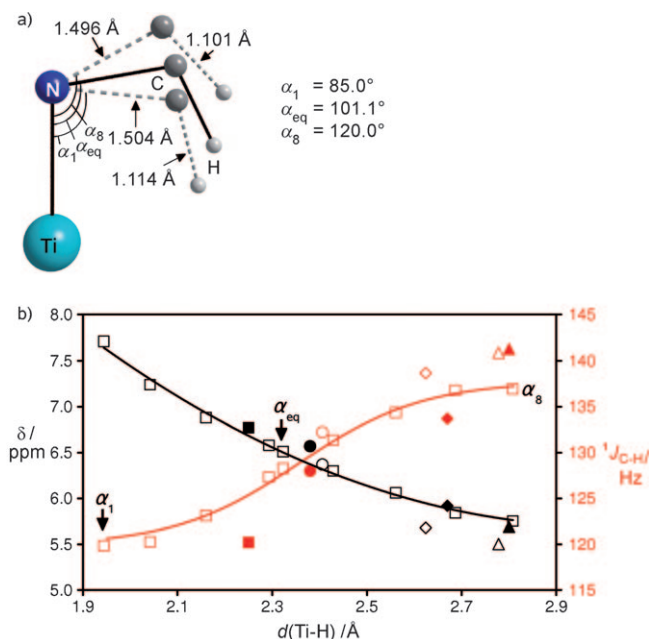


Figure 2. a) Superposition of the {TiNC_βH_β} fragments obtained from a scan of the relaxed PES scan ($\alpha_{1,\text{initial}} = 85^\circ$ and $\alpha_{8,\text{final}} = 120^\circ$; $\Delta = 5^\circ$) and the equilibrium geometry ($\alpha_{\text{eq}} = 101.1^\circ$) of **2**; b) correlation diagram of the chemical shift δ [ppm] of the agostic proton (black) and the $^1J_{C-H}$ coupling constant [Hz] (red) versus the Ti-H separation [Å] as obtained from the scan of the relaxed PES scan of **2** (squares); triangles **4**, diamonds **5**, and circles **6**. Filled symbols represent the respective experimental values. The lines are fits to the calculated data (δ values: black; $^1J_{C-H}$ values: red) of **2**.

Table 1: NMR chemical shifts (δ) [ppm], diamagnetic (σ^d) and paramagnetic (σ^p) shielding contributions, and the coupling constants $^1J_{\text{C-H}}$ [Hz] as obtained from the scan of the relaxed PES scan of the Ti-N-C angle in **2** and the experimental values of the benchmark systems.^[a]

Compd	$\angle \text{TiNC}_\beta$ [°]	d(Ti-H) [Å]	δ [ppm]	σ^d [ppm]	σ^p [ppm]	$^1J_{\text{C-H}}$ [Hz]
2 ^{exp}	100.4(1)	2.25(3)	6.77 ^[a]	—	—	120.2 ^[b]
2 ^{calcd}	85.0	1.944	7.71	30.11	-6.48	119.8
	101.1	2.323	6.51	29.25	-4.43	128.3
	115.0	2.687	5.84	29.04	-3.55	136.8
4 ^{exp}	117.4(2)	2.80(2)	5.69	—	—	141.3 ^[c]
4 ^{calcd}	118.1	2.778	5.50	28.55	-2.72	140.9
5 ^{exp}	114.2(2)	2.67(3)	5.92	—	—	133.7
5 ^{calcd}	113.3	2.624	5.68	28.98	-3.32	138.8
6 ^{exp}	104.5(1)	2.38(2)	6.57	—	—	128
6 ^{calcd}	104.5	2.406	6.37	28.93	-3.96	132.2

[a] ($\delta = \sigma(\text{TMS}) - \sigma$; with $\sigma^{\text{calcd}}(\text{TMS}) = 31.34$ ppm). Benchmark systems: $[\{\eta^5\text{-C}_5\text{H}_4\text{SiMe}_2\text{N}(\text{iPr})\}\text{TiCl}_2]$ (**4**; Ref. [9a]), $[\{\eta^5\text{-C}_5\text{H}_4(\text{CH}_2)_2\text{N}(\text{iPr})\}\text{TiCl}_2]$ (**5**; Ref. [9b]) and $[\{\eta^5\text{-C}_5\text{H}_4(\text{CH}_2)_2\text{N}(\text{iPr})\}\text{TiCl}_2]$ (**6**; Ref. [9b]). For further information see the Supporting Information. [b] At 178 K in $[\text{D}_8]\text{toluene}$. [c] Personal communication by J. Okuda.

for the agostic protons are surprisingly due to the dominant paramagnetic deshielding, σ^p (Table 1). The diamagnetic shielding, σ^d , shows the expected trend but increases only slightly with decreasing Ti \cdots H β distances. Furthermore, this small high-field shift is not supported by a significantly increasing negative atomic charge^[10] of the agostic proton (see the Supporting Information). Hence, classical arguments fail to explain this shift which is, however, more than overcompensated by the reverse paramagnetic deshielding contribution.^[11] Thus, our theoretical analysis of the NMR shielding tensor provides the basis of an explanation for the unusual downfield shift of the agostic protons in agostic d⁰ systems.^[12,9c,d]

Thus, the agostic protons in **2** and **3** are both characterized by downfield shifts which correlate with the M \cdots H distances. In contrast, the computed $^1J_{\text{C-H}}$ values which provide a reliable measure of the C-H activation^[2f,13] show a more complex dependency on the M \cdots H separation in agostic moieties. Hence, we suggest that the correlation between the M \cdots H distances and ^1H chemical shifts can be exploited as an experimental technique for the direct determination of M-H bond lengths and is an alternative to measuring the T_1 relaxation time in solution NMR measurements or to neutron diffraction studies of solids.^[14]

The previously discussed redistribution of the bonding electron density can be further analyzed by a topological analysis of the charge-density distribution $\rho(\mathbf{r})$. This analysis reveals the formation of an atomic interaction line between Ti and H β at $\angle \text{TiNC}_\beta$ angles smaller than 90°; this line signals increased Ti-H bonding (Figure 3). The increase of Ti-H bonding interactions is also reflected by the changes in the fine structure of the negative Laplacian, $L(\mathbf{r}) = -\nabla^2\rho(\mathbf{r})$, in the valence shell of charge concentration (VSCC)^[15] of the Ti atom. The local zone of charge depletion (CD), which faces the agostic H atom, provides a measure of the local Lewis acidity of the Ti atom and promotes the slight activation of the C-H β bond.^[2c,3e] It is noteworthy, that the fine structure of $L(\mathbf{r})$ closely resembles the ELF envelope maps^[16] drawn at a value of 0.84 (Figure 3). This result again reinforces the usefulness of $L(\mathbf{r})$ as an electron localization function and a

tool to locate regions of increased Lewis acidity at metal centers.^[17] The PES scan shows that this CD zone vanishes with decreasing Ti \cdots H distances, in agreement with a strengthening of the Ti \cdots H β -C interactions. We also note, that the charge concentration (CC) at the H atom shows a polarization towards the Lewis acidic metal atom at $\angle \text{TiNC}_\beta$ angles of 85° and below. As previously indicated, the extent of local Lewis acidic character at the metal atom appears to be a salient control parameter for β -H activation^[2c] in both amido and alkyl complexes containing agostic

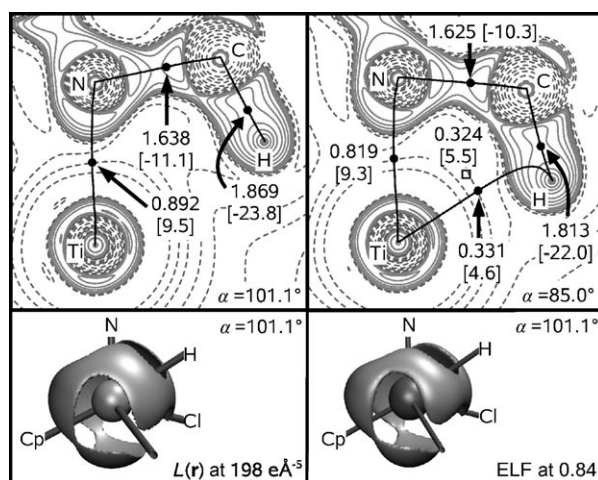


Figure 3. Top: Contour maps of $L(\mathbf{r}) = -\nabla^2\rho(\mathbf{r})$ containing the bond path (black solid line) in the Ti-N-C plane as obtained for the DFT-optimized structure of **2** with a $\angle \text{TiNC}_\beta$ angle of $\alpha = 101.1^\circ$ (left) and with α constrained to 85° (right). Values of $\rho(\mathbf{r})$ and $\nabla^2\rho(\mathbf{r})$ (square brackets) at the critical points are given in $\text{e}\text{\AA}^{-3}$ and $\text{e}\text{\AA}^{-5}$, respectively. Bond critical points (●), ring critical points (□). Positive (solid) and negative (dashed) contour lines are drawn at $0, \pm 2.0 \times 10^n, \pm 4.0 \times 10^n, \pm 8.0 \times 10^n \text{ e}\text{\AA}^{-5}$ with $n = \pm 3, \pm 2, \pm 1$; extra level at $191 \text{ e}\text{\AA}^{-5}$. Bottom: Envelope maps of $L(\mathbf{r})$ (left) and ELF (right) in the valence region of the Ti atom as obtained for the optimized geometry of **2**.

interactions—provided steric congestion does not prevent the formation of these interactions. However, the Ti \cdots H β interaction in the d⁰ complexes **2** and **3** is weak and should rather be interpreted as secondary interaction^[2c] which does not represent the major driving force behind the agostic phenomenon. Furthermore, the short M \cdots H β C β contacts in **2** are clearly enforced by the steric demand of the (iPr₂N) and Cp ligands. As a consequence, the DFT optimized geometries of $[\text{CpTi}(\text{Me}_2\text{N})\text{Cl}_2]$ (**2a**) and $[\text{Ti}(\text{Me}_2\text{N})\text{Cl}_3]$ (**2b**) display significantly larger $\angle \text{TiNC}_\beta$ angles and longer Ti \cdots H β contacts (**2a**: 2.596 Å; **2b**: 2.739 Å) than **2**.

In conclusion, on the basis of our phenomenological definition of β -agostic interactions, we suggest that both the d⁰

amido complex **2** and alkyl complex **3** can be classified as agostic. However, the driving force behind this phenomenon is different in both cases. Therefore, we suggest that agostic interactions in amido and alkyl d⁰ complexes should be discriminated from one another. Agostic interactions in alkyl d⁰ complexes are driven by negative hyperconjugative delocalization of the M–C bonding electron pair over the alkyl backbone.^[2c,f,3c,12,18] The rather modest secondary M···H–C interactions observed in each case are thus a consequence of the agostic distortion rather than its primary cause.^[2c] This process is clearly reflected by an increased olefinic character of the C_α–C_β bond. In contrast, the π-character of the M–N bond in the corresponding d⁰ amido complexes hinders such hyperconjugative delocalization of the M–N bonding electron pair. These systems display activated N_α–C_β bonds and might thus represent model systems for catalytic reactions involving the cleavage of the N_α–C_β bonds. This process may be driven by the formation of imido complexes displaying strong M=N bonds; for example, during the catalytic carboamination of alkynes with imines.^[19] Accordingly, our calculations show (Figure 2a) that the N_α–C_β bond lengths in **2** increase and become more activated with decreasing ∠TiNC_β angles and shorter M···H distances. These findings might therefore explain why β-H elimination processes are hindered in late-transition-metal amido complexes and are even unknown yet for d⁰ amido complexes.

Received: September 29, 2009

Published online: February 24, 2010

Keywords: agostic interactions · coordination chemistry · N ligands · NMR spectroscopy · transition metals

- [1] a) J. F. Hartwig, *J. Am. Chem. Soc.* **1996**, *118*, 7010–7011; b) Y.-C. Tsai, M. J. A. Johnson, D. J. Mindiola, C. C. Cummins, W. T. Klooster, T. F. Koetzle, *J. Am. Chem. Soc.* **1999**, *121*, 10426–10427; c) H. Cai, T. Chen, X. Wang, A. J. Schultz, T. F. Koetzle, Z. Xue, *Chem. Commun.* **2002**, 230–231; d) A. Dimitrov, S. Seidel, K. Seppelt, *Eur. J. Inorg. Chem.* **1999**, 95–99; e) P. Berno, S. Gambarotta, *Organometallics* **1995**, *14*, 2159–2161; f) L. Scoles, K. B. Rupp, S. Gambarotta, *J. Am. Chem. Soc.* **1996**, *118*, 2529–2530; g) I. De Castro, M. V. Galakhov, M. Gomez, P. Gomez-Sal, P. Royo, *Organometallics* **1996**, *15*, 1362–1368; h) K. Most, N. C. Mösch-Zanetti, D. Vidović, J. Magull, *Organometallics* **2003**, *22*, 5485–5490; i) K. W. Chiu, R. A. Jones, G. Wilkinson, A. M. R. Galas, M. B. Hursthouse, *J. Chem. Soc. Dalton Trans.* **1981**, 2088–2097; j) H. E. Bryndza, W. C. Fultz, W. Tam, *Organometallics* **1985**, *4*, 939–940; k) I. Matas, J. Cámpora, P. Palma, E. Álvarez, *Organometallics* **2009**, *28*, 6515–6523.
- [2] a) M. Brookhart, M. L. H. Green, *J. Organomet. Chem.* **1983**, *250*, 395–408; b) M. Brookhart, M. L. H. Green, L.-L. Wong, *Prog. Inorg. Chem.* **1988**, *36*, 1–124; For Reviews see c) W. Scherer, G. S. McGrady, *Angew. Chem.* **2004**, *116*, 1816–1842; *Angew. Chem. Int. Ed.* **2004**, *43*, 1782–1806; d) E. Clot, O. Eisenstein, *Struct. Bonding (Berlin)* **2004**, *113*, 1–36; e) M. Brookhart, M. L. H. Green, G. Parkin, *Proc. Natl. Acad. Sci. USA* **2007**, *104*, 6908–6914; f) M. Etienne, J. E. McGrady, F. Maseras, *Coord. Chem. Rev.* **2009**, *253*, 635–646.
- [3] a) R. M. Pupi, J. N. Coalter, J. L. Petersen, *J. Organomet. Chem.* **1995**, *497*, 17–25; b) **2** was synthesized according to modified literature methods (see Ref. [3a] and the Supporting Information); Crystal Data for **2** at 9(2) K: *M*_r = 284.07, with MoK_α radiation (0.71073 Å): triclinic, space group *P* $\bar{1}$ (No. 2), *a* = 7.9517(4), *b* = 9.2536(5), *c* = 9.4349(5) Å, *α* = 106.381(4), *β* = 99.880(5), *γ* = 91.053(4)°, *V* = 654.54(6) Å³, *Z* = 2, *θ* = 3.35 to 25.0°, 5558 reflections collected, 1816 independent reflections [*R*_{int} = 0.021], *μ* = 1.031 mm^{−1}, 212 parameters, goodness of fit 1.163, *R*1(*I* > 2σ) = 0.0274, *wR*2(all data) = 0.0631, largest diff. peak and hole 0.29 and −0.21 e Å^{−3}. For further information see the Supporting Information. CCDC 749125 and 749126 (studies at 100 K and 9 K) contain the supplementary crystallographic data for this paper. These data can be obtained free of charge from The Cambridge Crystallographic Data Centre via www.ccdc.cam.ac.uk/data_request/cif; c) W. Scherer, P. Sirsch, D. Shorokhov, M. Tafipolsky, G. S. McGrady, E. Gullo, *Chem. Eur. J.* **2003**, *9*, 6057–6070.
- [4] See for example, a) E. W. Jandciu, J. Kuzelka, P. Legzdins, S. J. Rettig, K. M. Smith, *Organometallics* **1999**, *18*, 1994–2004; b) J. M. Tanski, G. Parkin, *Organometallics* **2002**, *21*, 587–589.
- [5] This difference in the N–C1 and N–C2 bond lengths is also observed at 100 K (1.497(5)/1.481(5) Å, Ref. [3b]) and at room temperature (1.499(4)/1.480(4) Å, Ref. [3a]).
- [6] a) ADF2008.01e, SCM, Theoretical Chemistry, Vrije Universiteit, Amsterdam, The Netherlands, <http://www.scm.com>; b) G. te Velde, F. M. Bickelhaupt, S. J. A. van Gisbergen, C. Fonseca Guerra, E. J. Baerends, J. G. Snijders, T. Ziegler, *J. Comput. Chem.* **2001**, *22*, 931–967, and references therein.
- [7] W. Scherer, T. Priermeier, A. Haaland, H. V. Volden, G. S. McGrady, A. J. Downs, R. Boese, D. Bläser, *Organometallics* **1998**, *17*, 4406–4412.
- [8] Frequency calculations confirm that the ν(C–H) frequencies of both methine groups in **2** are virtually decoupled owing to the large mass difference between the CH₃ groups and the methine hydrogen atoms and can thus be employed as isolated reference stretching frequencies; a) D. C. McKean, *Chem. Soc. Rev.* **1978**, *7*, 399–422; b) D. C. McKean, *Croat. Chem. Acta* **1988**, *61*, 447–461; c) D. C. McKean, *J. Mol. Struct.* **1984**, *113*, 251–266; d) D. C. McKean, G. S. McGrady, A. J. Downs, W. Scherer, A. Haaland, *Phys. Chem. Chem. Phys.* **2001**, *3*, 2781–2794.
- [9] a) J. Okuda, T. Eberle, T. P. Spaniol, *Chem. Ber.* **1997**, *130*, 209–215; b) P.-J. Sinnema, L. van der Veen, A. L. Spek, N. Veldman, J. H. Teuben, *Organometallics* **1997**, *16*, 4245–4247; c) H. Nöth, M. Schmidt, *Organometallics* **1995**, *14*, 4601–4610; d) K. Ma, W. E. Piers, Y. Gao, M. Parvez, *J. Am. Chem. Soc.* **2004**, *126*, 5668–5669.
- [10] R. W. F. Bader, P. M. Beddall, *J. Chem. Phys.* **1972**, *56*, 3320–3329.
- [11] Thus, our study shows that high-field ¹H NMR chemical shifts appear to be only a characteristic feature of transition-metal complexes in low oxidation states where a positive paramagnetic shielding of the proton is dominant and complements the diamagnetic shielding; See, a) Y. Ruiz-Morales, G. Schreckenbach, T. Ziegler, *Organometallics* **1996**, *15*, 3920–3923; b) A. D. Buckingham, P. J. Stephens, *J. Chem. Soc.* **1964**, 2747–4583.
- [12] A. Haaland, W. Scherer, K. Ruud, G. S. McGrady, A. J. Downs, O. Swang, *J. Am. Chem. Soc.* **1998**, *120*, 3762–3772.
- [13] See, for example, X. Solans-Monfort, O. Eisenstein, *Polyhedron* **2006**, *25*, 339–348.
- [14] See, for example, a) W. Scherer, G. Eicklerling, M. Tafipolsky, G. S. McGrady, P. Sirsch, N. P. Chatterton, *Chem. Commun.* **2006**, 2986–2988; b) G. S. McGrady, P. Sirsch, N. P. Chatterton, A. Ostermann, C. Gatti, S. Altmannshofer, V. Herz, G. Eicklerling, W. Scherer, *Inorg. Chem.* **2009**, *48*, 1588–1598.
- [15] R. F. W. Bader et al. have demonstrated that the negative Laplacian of the charge-density distribution, *L*(**r**) = −∇²ρ(**r**), determines where the charge-density distribution is locally concentrated (*L*(**r**) > 0) or locally depleted (*L*(**r**) < 0) in the valence shell of charge concentration; a) R. F. W. Bader, P. J. MacDougall, C. D. H. Lau, *J. Am. Chem. Soc.* **1984**, *106*, 1594–

- 1605; b) R. F. W. Bader, H. Essén, *J. Chem. Phys.* **1984**, *80*, 1943–1960.
- [16] a) A. D. Becke, K. E. Edgecombe, *J. Chem. Phys.* **1990**, *92*, 5397–5403; b) M. Kohout, A. Savin, *Int. J. Quantum Chem.* **1996**, *60*, 875–882.
- [17] a) G. S. McGrady, A. Haaland, H. P. Verne, H. V. Volden, A. J. Downs, D. Shorokhov, G. Eickerling, W. Scherer, *Chem. Eur. J.* **2005**, *11*, 4921–4934; b) R. W. F. Bader, S. Johnson, T. H. Tang, P. L. A. Popelier, *J. Phys. Chem.* **1996**, *100*, 15398–15415; c) F. R. Wagner, M. Kohout, Y. Grin, *J. Phys. Chem. A* **2008**, *112*, 9814–9828.
- [18] a) W. Scherer, P. Sirsch, M. Grosche, M. Spiegler, S. A. Mason, M. G. Gardiner, *Chem. Commun.* **2001**, 2072–2073; b) W. Scherer, P. Sirsch, D. Shorokhov, G. S. McGrady, S. A. Mason, M. Gardiner, *Chem. Eur. J.* **2002**, *8*, 2324–2334; c) L. Perrin, L. Maron, O. Eisenstein, M. F. Lappert, *New J. Chem.* **2003**, *27*, 121–127; d) D. A. Pantazis, J. E. McGrady, M. Besora, F. Maseras, M. Etienne, *Organometallics* **2008**, *27*, 1128–1134; e) M. P. Mitoraj, A. Michelak, T. Ziegler, *Organometallics* **2009**, *28*, 3727–3733.
- [19] a) F. Basuli, H. Aneetha, J. C. Huffman, D. J. Mindiola, *J. Am. Chem. Soc.* **2005**, *127*, 17992–17993; b) H. Aneetha, F. Basuli, J. Bollinger, J. C. Huffman, D. J. Mindiola, *Organometallics* **2006**, *25*, 2402–2404. Direct cleavage of (more polar) Si–N bonds—which represents an α -elimination process—has been observed in silylamido complexes c) W. A. Herrmann, W. Baratta, *J. Organomet. Chem.* **1996**, *506*, 357–361.
-